Theoret. Appl. Mech., Vol.39, No.3, pp. 209–231, Belgrade 2012

Pulsatile flow of shear-dependent fluid in a stenosed artery

Mani Shankar Mandal* **Swati Mukhopadhyay†** **G. C. Layek‡**

Abstract

This paper aims to investigate the blood flow in a bell-shaped constricted rigid tube, modeled as stenosed artery. The flow is assumed to be axi-symmetric, laminar and of oscillatory type. A mathematical model of shear-thinning fluid corresponding to the shear-dependent blood viscosity (mainly due to the behavior of the red blood cells in suspension of the flowing blood) is considered. The governing equations of motion are presented with the help of stream function-vorticity and are solved numerically by finite-difference technique. The shear-thinning fluid model for the flowing blood has significant contribution in the dynamics of oscillatory blood flow. The results reveal that the arterial wall shear stress reduced significantly and the peak value of the wall shear stress at the maximum area reduction is comparatively low for Newtonian fluid viscosity. The lengths of recirculating regions formed after the constriction are reduced for the shear-thinning blood viscosity model and also for its different material parameters.

Keywords: Pulsatile flow, shear-dependent viscosity, bell-shaped constriction.

*Department of Mathematics, Krishnagar Govt. College, Krishnagar, Nadia-741101, West Bengal, India, e-mail: manimath@yahoo.com

†Department of Mathematics, The University of Burdwan, Burdwan-713104, West Bengal, India

‡Department of Mathematics, The University of Burdwan, Burdwan-713104,West Bengal, India

1 Introduction

Of late, the study of bio-fluid dynamics has become quite interesting to many researchers from theoretical, experimental as well as clinical point of view. Flow through arteries becomes complicated by the formation of atherosclerotic plaques on the arterial wall which impede the flow through the artery and which may substantially affect the wall shear stress distribution. The blockage in the coronary artery passage area has severe impact in blood flow leading to the malfunction of the cardiovascular system. The development of artheriosclerosis is known to be closely related with the presence of a locally irregular flow pattern, variation of arterial wall shear stress and also the boundary layer flow separation. The exact mechanism responsible for the initiation of such arterial constriction (stenosis) is not clearly known, but their effects on the resulting flow dynamics are quite significant, in human circulatory system.

Several investigations on flow through stenosed artery have been carried out to evaluate the flow characteristics under steady and pulsatile flow conditions. Attention is also given to study experimentally steady and unsteady flows across a stenosis which can be found in Young & Tsai [1], [2] and in Siouffi et al. [3]. In fact, blood is a complex rheological mixture showing several non-Newtonian properties, shear-thinning, yield stress, stress relaxation etc. The rheological properties of fluid have important influences on wall shear stress, oscillatory shear index etc. So it is very important to address the significance of non-Newtonian models for the purpose of reliable hemodynamical modeling.

Blood may be considered as a Newtonian fluid for the flow within the heart and the aorta of the human cardiovascular system. For blood flow in smaller arteries of diameter 0.5mm, a simple rescaling of the Newtonian viscosity is sufficient to take account of non-Newtonian behavior of blood (Ku [4], Caro et al. [5]). But in particular situations blood may behave as a non-Newtonian fluid, even in large arteries, as reported in Nakamura and Sawada [6]. Under diseased conditions, blood exhibits remarkable non-Newtonian properties.

Extensive theoretical and experimental research works on fluid dynamics through differently geometries have been carried out to evaluate the flow pattern and the wall shear stress under steady and pulsatile flow conditions. The nonlinear separated vorticity modifies the boundary layer structure and its separation region which eventually changes the whole flow dynamics. The

dynamics of this kind of steady and pulsatile flow phenomena through a modeled stenosed artery and the corresponding flow separation has been studied in detailed by several researchers viz. Layek and Midya [7], Pedrizzetti [8], Siouuffi et al. [3]), Mittal et al. [9], Tutty [10], Tutty and Pedley [11]. Several physical quantities have been proposed in literature in order to measure the risk zones in blood vessel. Observations show that one reason behind this is the oscillatory nature of the blood flow during the diastolic phase at every single heart beat.

Number of researchers have studied flow of non-Newtonian fluids through arterial stenosis. Best of the authors' knowledge, only a few of them take into account both the unsteadiness and non-Newtonian effects. Thus there is much left to be studied with the simultaneous effect of physiological pulsatile flow and non-Newtonian behaviour of blood in presence of stenosis. In the present work, a numerical investigation concerning axi-symmetric pulsatile blood flow through a bell-shaped stenosed rigid artery having a medium degree of contraction is carried out. The assumption of wall rigidity may not seriously affect the flow since the development of atherosclerosis in arteries causes a significant reduction in the distensibility of its wall as is evident from the observation of Nerem[12]. A shear thinning blood viscosity model is considered. The rheological parameters involved in the blood flow are investigated, in details. The sinusoidal and physically relevant pulsations are used for this study applicable to smaller arterial flow.

2 Mathematical model for blood viscosity

The viscosity of blood depends on the viscosity of plasma and its protein content, the haematocrit, the temperature, the shear rate and the narrowness of the blood vessel. Among these, the blood viscosity is mainly influenced by three factors: hematocrit, temperature and flow rate. In this paper we consider that the viscosity of streaming blood is depending on the shear-rate, that is, the streaming blood is a shear-thinning fluid. It is experimentally shown that the apparent viscosity of blood decreases as the shear-rate increases. In recent past, many constitutive equations have been proposed for the blood to model this shear-thinning property (Anand and Rajagopal [13], Yeleswarapu et al. [14]).

The shear dependent viscosity of Yeleswarapu [15] is given as

$$\mu(\dot{\gamma}) = \eta_\infty + (\eta_0 - \eta_\infty)\frac{[1 + \log_e(1 + \Lambda\dot{\gamma})]}{1 + \Lambda\dot{\gamma}}, \tag{1}$$

where η_0 and η_∞ ($\eta_0 \geq \eta_\infty$) are the asymptotic apparent viscosities as $\dot{\gamma} \to 0$ and ∞ respectively, and $\Lambda \geq 0$ is a material constant having the dimension of time and representing the degree of shear thinning (for $\eta_0 = \eta_\infty$, $\mu(\dot{\gamma})$ =constant and the model reduces to the Newtonian one).

According to Yeleswarapu et al. [14] the physiological values for the blood are taken asλ=14.72 and Λ=14.81. These physiological values for blood are taken throughout the present study except where the variation are performed. The Fig. 1(a) and (b) represent the behaviour of viscosity of blood due to change in physiological values.

2.1 Shape of the arterial stenosis

Arterial constriction is asymmetric and irregular in shape containing many ups and downs. In general, the surface irregularities of the stenosis add complexity to experimental and numerical simulations of the flow phenomena. Keeping in view of such complexities, in the present investigation we have taken a simple bell-shaped constriction. The rigid tube modeled as artery has a circular cross section whose radius is R_0 everywhere except in a small region centered at z=0, with a mild smooth axi-symmetric contraction, as represented by equation:

$$r_0\,(z) = 1 - \delta e - \sigma z^2, \tag{2}$$

where 0$\leq\delta$¡1 is a measure of the degree of contraction,$\sigma$is its length. For a slowly varying smooth profile, $\sigma$is kept small. The geometry of the tube with bell-shaped constriction has been presented in Fig. 2.

3 Flow Analysis

Consider the pulsatile flow of an incompressible viscous fluid, with constant density ρ and shear dependent viscosity $\mu(\dot{\gamma})$ moving in an axi-symmetric tube (modeled as artery) with a bell-shaped constriction (axi-symmeric). We assume the axis as the z-axis of a cylindrical system of coordinates(r^*, z^*, θ^*). The axial symmetry makes the flow independent fromθ^*. Let R_0 be the

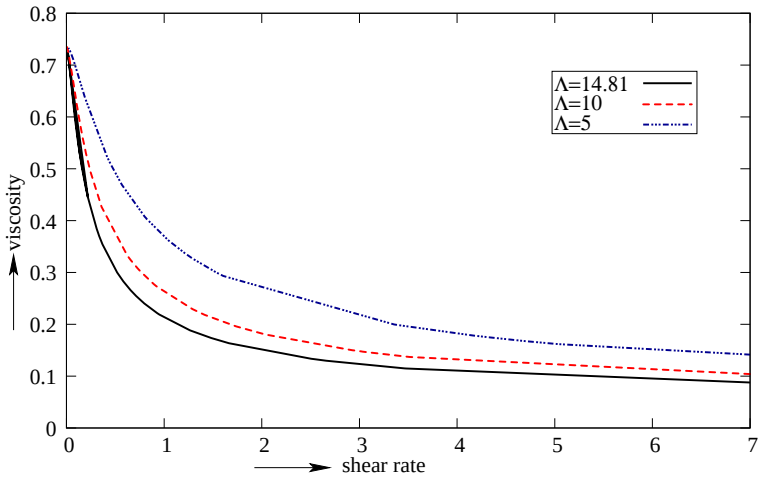

(a) Variation of Λ.

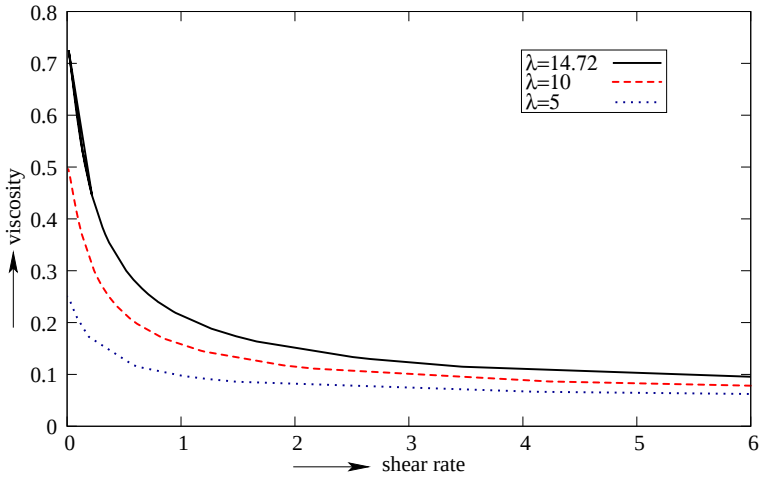

(b) Variation of λ.

Figure 1: Viscosity function for shear dependent model for the variation of the parameter λ and Λ.

radius of the tube in the unocculated portion and $r_0^*(z^*)$ define the wall of the vascular tube. The origin O is taken at the inlet. For pulsatile flow condition, the mean velocity at the inlet will be time-dependent and hence the fluid is moving inside the tube with a pulsatile flow volume rate which is

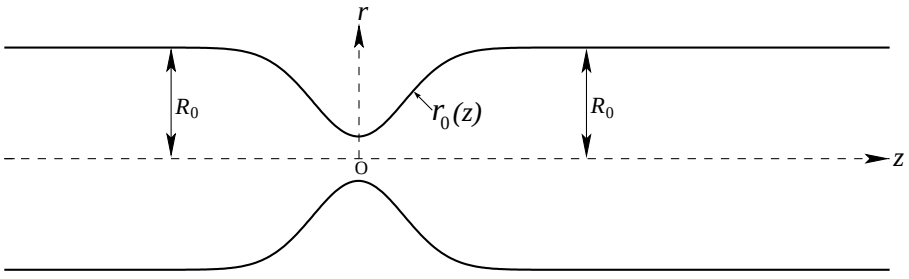

Figure 2: Schematic diagram of the rigid tube with bell-shaped constriction.

prescribed at a particular location (i.e. at the inlet of the tube) as

$$Q^*(t^*) = \frac{\pi}{2} R_0^2 U_0 \left[1 + \sin\left(2\pi \frac{t^*}{T}\right)\right], \tag{3}$$

where U_0 is maximum value (in period) of the cross-sectionally averaged velocity at the tube inlet and T is the period of pulsation of the flow under the approximation of the axial symmetry. The following dimensionless quantities in this axi-symmetric two-dimensional flow are given below

$$z = \frac{z^*}{R_0}, r = \frac{r^*}{R_0}, r_0 = \frac{r_0^*}{R_0}, u = \frac{u^*}{U_0}, v = \frac{v^*}{U_0}, t = \frac{t^*}{T}, p = \frac{p^*}{\rho U_0^2}, \lambda = \frac{\eta_0}{\eta_\infty}, \tag{4}$$

where p^* is the pressure, u^* and v^* are the velocity components along z^* and r^*-axes, respectively.

The unsteady two dimensional Navier-Stokes equation of an incompressible fluid with shear dependent viscosity may be written in dimensionless form as:

$$\begin{aligned} st\frac{\partial u}{\partial t} + \frac{\partial uv}{\partial r} + \frac{\partial u^2}{\partial z} + \frac{uv}{r} = &- \frac{\partial p}{\partial z} + \frac{1}{Re}\left[\mu_1\left\{\frac{\partial^2 u}{\partial r^2} + \frac{1}{r}\frac{\partial u}{\partial r} + \frac{\partial^2 u}{\partial z^2}\right\}\right. \\ &\left. + \frac{\partial \mu_1}{\partial r}\left\{\frac{\partial u}{\partial r} + \frac{\partial v}{\partial z}\right\} + 2\frac{\partial \mu_1}{\partial z}\frac{\partial u}{\partial z}\right], \end{aligned} \tag{5}$$

$$\begin{aligned} st\frac{\partial v}{\partial t} + \frac{\partial v^2}{\partial r} + \frac{\partial uv}{\partial z} + \frac{v^2}{r} = &- \frac{\partial p}{\partial r} + \frac{1}{Re}\left[\mu_1\left\{\frac{\partial^2 v}{\partial r^2} + \frac{1}{r}\frac{\partial v}{\partial r} + \frac{\partial^2 v}{\partial z^2} - \frac{v}{r^2}\right\}\right. \\ &\left. + 2\frac{\partial \mu_1}{\partial r}\frac{\partial v}{\partial r} + \frac{\partial \mu_1}{\partial z}\left(\frac{\partial v}{\partial z} + \frac{\partial u}{\partial r}\right)\right], \end{aligned} \tag{6}$$

and

$$r\frac{\partial u}{\partial z}+\frac{\partial vr}{\partial r}=0, \tag{7}$$

where $Re=U_0R_0/\nu$ is the flow Reynolds number and $st=R_0/U_0T$ is the Strouhal number and $\mu_1=1+(\lambda-1)\frac{[1+\log_e(1+\Lambda\dot{\gamma})]}{1+\Lambda\dot{\gamma}}$ is the dimensionless fluid viscosity with

$$\dot{\gamma}=\left[2\left(\frac{\partial u}{\partial z}\right)^2+2\left(\frac{\partial v}{\partial r}\right)^2+2\left(\frac{v}{r}\right)^2+\left(\frac{\partial u}{\partial r}+\frac{\partial v}{\partial z}\right)^2\right]^{\frac{1}{2}}. \tag{8}$$

We now define the dimensionless Stokes stream function $\psi(z,r,t)$as follows,

$$u=\frac{1}{r}\frac{\partial\psi}{\partial r}, v=-\frac{1}{r}\frac{\partial\psi}{\partial z} \tag{9}$$

and the corresponding azimuthal vorticity function $\omega(z,r,t)$as

$$\omega=\frac{\partial v}{\partial z}-\frac{\partial u}{\partial r}. \tag{10}$$

Using (9) and (10) and by cross-differentiation of the momentum equation (5) and (6) the pressure term is eliminated and we have the following usual coupled equations for stream function and vorticity transport

$$-\omega r=\frac{\partial^2\psi}{\partial z^2}+\frac{\partial^2\psi}{\partial r^2}-\frac{1}{r}\frac{\partial\psi}{\partial r}, \tag{11}$$

$$\begin{aligned} st\frac{\partial\omega}{\partial t}+u\frac{\partial\omega}{\partial z}+v\frac{\partial\omega}{\partial r}-\frac{v\omega}{r}=\frac{1}{Re}\Bigg[&\mu_1\left(\frac{\partial^2\omega}{\partial z^2}+\frac{\partial^2\omega}{\partial r^2}+\frac{1}{r}\frac{\partial\omega}{\partial r}-\frac{\omega}{r^2}\right)\\ &+2\frac{\partial\mu_1}{\partial z}\frac{\partial\omega}{\partial z}+\frac{\partial\mu_1}{\partial r}\left(2\frac{\partial\omega}{\partial r}+\frac{\omega}{r}\right)\\ &-2\frac{\partial^2\mu_1}{\partial r\partial z}\left(\frac{v}{r}+2\frac{\partial u}{\partial z}\right)\\ &+\left(\frac{\partial^2\mu_1}{\partial z^2}-\frac{\partial^2\mu_1}{\partial r^2}\right)\left(\frac{\partial u}{\partial r}+\frac{\partial v}{\partial z}\right)\Bigg]. \end{aligned} \tag{12}$$

3.1 Boundary conditions for the flow problem

At the inlet cross-section of the tube, the flow is assumed to be fully developed, that is, $\partial\omega/\partial z = \partial\psi/\partial z = 0$and at the outlet cross-section, we have considered the flow field has no change which gives$\partial^2\omega/\partial z^2 = \partial^2\psi/\partial z^2 = 0$. A time dependent flow rate $Q(t)$ is given at the upper wall of the tube.

The flow symmetry gives the following conditions

$$\psi = 0, \;\; \omega = 0 \;\; \text{at } r = 0. \tag{13}$$

The conditions of 'no slip' at the tube wall requires that

$$\partial\psi/\partial z = 0 = \partial\psi/\partial r \;\; \text{at } r = r_0(z). \tag{14}$$

Since the mass flux across all cross-sections of the tube is same at any instant of time, so

$$\int_0^{r_0(z)} 2\pi r \left(\frac{1}{r}\frac{\partial\psi}{\partial r}\right) dr = Q(t). \tag{15}$$

This gives the value of the stream function ψ at $r = r_0(z)$ (the tube wall)

$$\psi(t) = Q(t)/2\pi \tag{16}$$

where the non-dimensional $Q(t) = \pi/2\,(1 + \sin(2\pi t))$ gives $\psi(t) = 0.25\,(1 + \sin 2\pi t)$.

The vanishing normal velocity component at the tube wall gives that the stream function is constant along the wall at particular instant of time and also the zero value of the tangential velocity implies that the first order normal derivative and the second order mixed derivative of the stream function are zero (Batchelor [16], Pedrizetti [8]). These conditions of the stream function when used in equation (11) provide the wall vorticity at the upper wall. Using these conditions for stream function, the wall vorticity at $r = r_0(z)$can be obtained which is most crucial in finding the flow quantities of the vorticity-stream function formulation.

We choose a suitable system of coordinates where the arterial constriction coincides with a constant coordinate curve. A coordinate transformation is used defining a new R-coordinate as$R = r/r_0(z)$.

The equations for stream function (11) and the vorticity transport equation (12) are transformed to the co-ordinate $(R, z, t)$and the transformed equations are not presented.

The transformed boundary conditions on the stream function ψ and vorticity ω at R=1 become

$$\psi\left(z, R=1, t\right) = 0.25\left(1+\sin 2\pi t\right) \tag{17}$$

$$\omega\left(z, R=1, t\right) = -\frac{1}{r_0^3}\left[1+\left(\frac{dr_0}{dz}\right)^2\right]\left(\frac{\partial^2\psi}{\partial R^2}\right)_{atR=1} \quad . \tag{18}$$

4 Numerical Method

The transformed governing equations together with the initial and boundary conditions are solved numerically by using finite difference technique. A very efficient implicit technique, viz. Alternating Direction Implicit (ADI) method has been used to solve vorticity transport equation which is parabolic in nature. The elliptic stream function equation is discretised using central difference formula and the algebraic system is solved by using SLOR algorithm (Successive Line Over relaxation Method), (Peyret and Taylor [17]).

The finite difference representations of the derivatives and all other terms have been written at the mesh point (j,k) which indicates a point where $z = j\Delta z$ and $R = k\Delta R$, Δz and ΔR being the increment of z and R, respectively. The finite difference form for time is written as $t = m\Delta t$, where Δt is the time increment and the superscript denotes the time direction. A tridiagonal system of algebraic equations associated with each line (constant j) in R-direction is formed. The finite-difference representation is given below

$$A(k)\psi_{j,k-1}^{m+1} + B(k)\psi_{j,k}^{m+1} + C(k)\psi_{j,k+1}^{m+1} = S(k) \tag{19}$$

where the quantities $A(k)$, $B(k)$, $C(k)$ and $S(k)$ are defined as

$$A(k) = \frac{M_2}{(\Delta R)^2} - \frac{M_1}{(2\Delta R)}$$

$$B(k) = -\frac{2}{(\Delta z)^2} - \frac{2M_2}{(\Delta R)^2}$$

$$C(k) = \frac{M_2}{(\Delta R)^2} + \frac{M_1}{(2\Delta R)}$$

$$S(k) = -r_0 R\omega_{j,k}^m - \frac{\psi_{j+1,k}^m - 2\psi_{j,k}^m + \psi_{j,k-1}^m}{(\Delta z)^2} + M_3\frac{\psi_{j+1,k+1}^m - \psi_{j+1,k-1}^m - \psi_{j-1,k+1}^m + \psi_{j-1,k-1}^m}{4\Delta z\Delta R}$$

and

$$M_1 = \frac{2R}{r_0^2}\left(\frac{dr_0}{dz}\right)^2 - \frac{R}{r_0}\frac{d^2r_0}{dz^2} - \frac{1}{Rr_0^2},$$

$$M_2 = \frac{R^2}{r_0^2}\left(\frac{dr_0}{dz}\right)^2 + \frac{1}{r_0^2},$$

$$M_3 = \frac{2R}{r_0}\frac{dr_0}{dz}$$

The tridiagonal system of equations can be solved by using well-known Thomas algorithm for each (constant j) in R-direction. The successive over relaxation scheme is used and the relaxation parameter is chosen 1.3 for the grid size 250 x 22.

An ADI method is used to obtain a numerical solution of the momentum equation subject to the boundary conditions. But the main difficulty with the stream function-vorticity formulation is to derive the boundary conditions for the vorticity. In our present computation, we obtain a second order accurate formula for wall vorticity from the equation represented by stream-function assuming the known values of the stream-function. The vorticity at the tube wall are given by

$$\omega(z, R=1, t) = -2r_0^3(j)\left[1 + \left(\frac{dr_0}{dz}\right)^2_{(j,kstp)}\right]\left(\frac{\psi_{j,kstp-1} - \psi_{j,kstp}}{(\Delta R)^2}\right) \qquad (20)$$

where k=kstp corresponds to the value of R at the boundary i.e. R=1. This necessitates the evaluation of ψ at a previous level iteration (or time) level.

The momentum equation is now written in two half time-steps with one spatial variable implicit in one half times-step and the other spatial variable implicit in the other half time-step. Thus each half step involves the direct solution of a tridiagonal system of equations. During the first half time-step, the value of the vorticity ω is known at time level m and unknown at the $(m+1/2)$. These unknown values,$\omega_{j,k}^{m+1/2}$ are associated with the R-direction (i.e., for R-implicit and z-explicit). The discretised version of momentum equation is given by

$$P(k)\omega_{j,k-1}^{m+1/2} + Q(k)\omega_{j,k}^{m+1/2} + R(k)\omega_{j,k+1}^{m+1/2} = S(k) \qquad (21)$$

where $P(k)$, $Q(k)$, $R(k)$and $S(k)$are given by

$$P(k) = \frac{1}{2\Delta R}\left(\frac{uR}{r_0}\frac{dr_0}{dz} - \frac{v}{r_0}\right) + \frac{\mu_1}{Re}\left(\frac{L_1}{2\Delta R} - \frac{L_2}{(\Delta R)^2}\right) - \frac{\partial \mu_1}{\partial z}\frac{R}{Rer_0\Delta R}\frac{dr_0}{dz}$$
$$+ \frac{1}{Rer_0^2\Delta R}\left(R^2\left(\frac{dr_0}{dz}\right)^2 + 1\right)\frac{\partial \mu_1}{\partial R},$$
$$Q(k) = \frac{2st}{\Delta t} + \frac{2\mu_1 L_2}{Re(\Delta R)^2} + \frac{\mu_1}{(Rr_0)^2 Re} - \frac{1}{Rr_0^2 Re}\frac{\partial \mu_1}{\partial R} - \frac{v}{Rr_0},$$
$$R(k) = -\frac{1}{2\Delta R}\left(\frac{uR}{r_0}\frac{dr_0}{dz} - \frac{v}{r_0}\right) - \frac{\mu_1}{Re}\left(\frac{L_1}{2\Delta R} + \frac{L_2}{(\Delta R)^2}\right) + \frac{\partial \mu_1}{\partial z}\frac{R}{Rer_0\Delta R}\frac{dr_0}{dz}$$
$$- \frac{1}{(Re)r_0^2\Delta R}\left(R^2\left(\frac{dr_0}{dz}\right)^2 + 1\right)\frac{\partial \mu_1}{\partial R},$$
$$S(k) = \frac{2st}{\Delta t}\omega_{j,k}^m - u\left(\frac{\omega_{j+1,k}^m - \omega_{j-1,k}^m}{2\Delta z}\right) + \frac{\mu_1}{Re}\left\{\left(\frac{\omega_{j+1,k}^m - 2\omega_{j,k}^m + \omega_{j-1,k}^m}{(\Delta z)^2}\right)\right.$$
$$\left. - \frac{R}{r_0}\frac{dr_0}{dz}\left(\frac{\omega_{j+1,k+1}^m - \omega_{j+1,k-1}^m - \omega_{j-1,k+1}^m + \omega_{j-1,k-1}^m}{2\Delta R\Delta z}\right)\right\}$$
$$+ \left(\frac{\partial \mu_1}{\partial z} - \frac{R}{r_0}\frac{dr_0}{dz}\frac{\partial \mu_1}{\partial R}\right)\left(\frac{\omega_{j+1,k}^m - \omega_{j-1,k}^m}{Re\Delta z}\right) + \frac{P_2}{Re}$$

and

$$L_1 = \frac{2R}{r_0^2}\left(\frac{dr_0}{dz}\right)^2 + \frac{1}{Rr_0^2} - \frac{R}{r_0}\frac{d^2r_0}{dz^2},$$
$$L_2 = \frac{R^2}{r_0^2}\left(\frac{dr_0}{dz}\right)^2 + \frac{1}{r_0^2},$$
$$P_2 = -2\left(\frac{1}{r_0}\frac{\partial^2 \mu_1}{\partial R\partial z} - \frac{1}{r_0^2}\frac{dr_0}{dz}\frac{\partial \mu_1}{\partial R} - \frac{R}{r_0^2}\frac{dr_0}{dz}\frac{\partial^2 \mu_1}{\partial R^2}\right)\left(\frac{v}{Rr_0} + 2\frac{\partial u}{\partial z}\right.$$
$$\left. - \frac{2R}{r_0}\frac{dr_0}{dz}\frac{\partial u}{\partial R}\right) + \left(\frac{\partial^2 \mu_1}{\partial z^2} - \frac{2R}{r_0}\frac{\partial^2 \mu_1}{\partial R\partial z}\frac{dr_0}{dz} + \left[\frac{2R}{r_0^2}\left(\frac{dr_0}{dz}\right)^2\right.\right.$$
$$\left.\left. - \frac{R}{r_0}\frac{d^2r_0}{dz^2}\right]\frac{\partial \mu_1}{\partial R}\right)\left(\frac{1}{r_0}\frac{\partial \mu_1}{\partial R} + \frac{\partial v}{\partial z} - \frac{R}{r_0}\frac{dr_0}{dz}\frac{\partial v}{\partial R}\right).$$

Equation (21) is tridiagonal system of algebraic equations which can be solved using well-known Thomas algorithm (Peyret and Taylor [17]).

To advance to the next half-step with the z-direction (i.e.,z-implicit and R-explicit), the following set of equations are solved for the unknown values

of $\omega_{j,k}^{m+1}$ using the known indeterminate values obtained in the previous half-level as

$$P(j)\omega_{j-1,k}^{m+1} + Q(j)\omega_{j,k}^{m+1} + R(j)\omega_{j,k+1}^{m+1} = S(j) \tag{22}$$

where the quantities $P(j)$, $Q(j)$, $R(j)$ and $S(j)$ are given by

$$P(j) = -\frac{u}{2\Delta z} - \frac{\mu_1}{Re(\Delta z)^2} + \left(\frac{\partial \mu_1}{\partial z} - \frac{R}{r_0}\frac{dr_0}{dz}\frac{\partial \mu_1}{\partial R}\right)\frac{1}{\Delta z Re}$$

$$Q(j) = \frac{2st}{\Delta t} - \frac{v}{r_0 R} + \frac{2\mu_1}{Re(\Delta z)^2} + \frac{\mu_1}{Rer_0^2 R^2} - \frac{\partial \mu_1}{\partial R}\frac{1}{Rer_0^2 R}$$

$$R(j) = \frac{u}{2\Delta z} - \frac{\mu_1}{Re(\Delta z)^2} - \left(\frac{\partial \mu_1}{\partial z} - \frac{R}{r_0}\frac{dr_0}{dz}\frac{\partial \mu_1}{\partial R}\right)\frac{1}{\Delta z Re}$$

$$\begin{aligned} S(j) = {} & \frac{2st}{\Delta t}\omega_{j,k}^{m+1/2} + \left\{\frac{uR}{r_0}\frac{dr_0}{dz} - \frac{v}{r_0} + \frac{L_1\mu_1}{Re} - \left(\frac{\partial \mu_1}{\partial z} - \frac{R}{r_0}\frac{dr_0}{dz}\frac{\partial \mu_1}{\partial R}\right)\frac{2R}{Rer_0}\frac{dr_0}{dz}\right. \\ & \left. + \frac{2}{Rer_0^2}\frac{\partial \mu_1}{\partial R}\right\}\left(\frac{\omega_{j,k+1}^{m+1/2} - \omega_{j,k-1}^{m+1/2}}{2\Delta R}\right) \\ & - \frac{R\mu_1}{r_0 Re}\frac{dr_0}{dz}\left(\frac{\omega_{j+1,k+1}^{m+1/2} - \omega_{j+1,k-1}^{m+1/2} - \omega_{j-1,k+1}^{m+1/2} + \omega_{j-1,k-1}^{m+1/2}}{2\Delta R\Delta z}\right) \\ & + \frac{L_2}{Re(\Delta R)^2}\left(\omega_{j,k+1}^{m+1/2} - 2\omega_{j,k}^{m+1/2} + \omega_{j,k-1}^{m+1/2}\right) + \frac{P_2}{Re}. \end{aligned}$$

After solving the system the vorticities at (m+1)th level are obtained in the computational plane.

4.1 Stability Criteria of the numerical scheme

Some restrictions have been incorporated on selecting time step Δt depending on the grid sizeΔz,ΔR. The first restrictions i.e., CFL (Courant, Friedrichs & Lewy) condition, is given as

$$\Delta t_1 \leq Min\left[\frac{\Delta z}{|u|}, \frac{\Delta R}{|v|}\right]_{(j,k)}$$

The second restriction related to the viscous effects and is given by

$$\Delta t_2 \leq Min\left[\frac{Re}{2}\frac{\Delta z^2 \Delta R^2}{(\Delta z^2 + \Delta R^2)}\right]_{(j,k)}$$

Actually, the time step is chosen by using the following relation

$$\Delta t = \beta Min\left[\Delta t_1, \Delta t_2\right],$$

where the minimum is taken in the global sense and the time steps Δt_1 and Δt_2 must satisfy the above two inequalities. For pulsatile flow, the parameterβ is selected 0.001 andΔt=0.0005.The different flow parameters involve in the present study are taken asRe=10 to150, st=0.06 to 0.09, σ=0.8, δ=0.3, λ=14.72 and Λ=14.81.

5 Results and Discussions

For the purpose of verification of the present numerical code, computations for the stream- function (ψ), vorticity (ω) in case of steady flow through a long circular straight tube for different values of R at the Reynolds number Re=10 and for Strouhal number st=1 with no-slip boundary condition for grid size 250 x 22 are made and found in excellent agreement with the exact values of ψ and ωas shown in Table-I. The wall shear stress distribution of a Newtonian fluid through a tube with single bell-shaped constriction centered at z=0 under steady flow rate condition for Re=10 has been presented in Fig.3. However, good agreement between the present simulation on Newtonian flow and that of G.Pontrelli [18] establishes the validity of the model under consideration together with the numerical code used.

An extensive quantitative analysis has been performed with the help of the present model of bell shaped constricted artery, for various physical quantities of major physiological relevance such as the wall shear stress, velocity profiles etc. through their graphical representations. We are mainly interested to study the effects of pulsatile flow and purely sinusoidal unsteady flow rate on such type of constriction. From clinical point of view, the results obtained in this study have important bearings on flow characteristics.

The stress on the wall of the artery plays an important role in the creation and proliferation of the arterial disease. The principal features of the flow can also be determined by examining the wall shear stress. High wall shear stress may damage the vessel wall and is the cause of the intimal thickening. On the other hand, the plaque formation in an artery develops in the regions of low arterial wall shear stress. Atherosclerotic lesions are associated with low and oscillatory wall shear stress. Experimental studies suggest that wall shear stress is higher on the outer wall of curvature, whereas it is low in

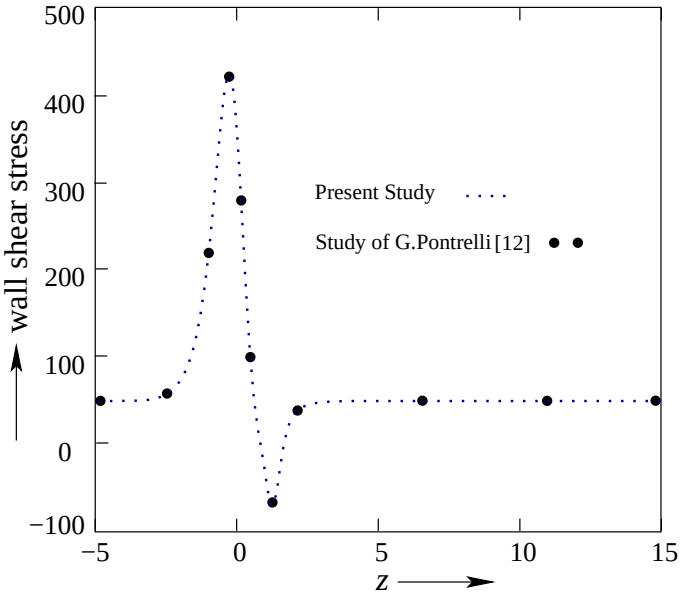

Figure 3: Comparison of wall shear stress in Newtonian case for Re=10 under steady flow condition.

the inner wall of curvature. In the aorta, atherosclerotic lesions occur along the inner wall of curvature where there is low shear stress. Cholesterol is actually synthesized in the arterial wall and diffuses in to the lumen where it is washed away by the blood stream. In the region of high wall shear stresses (and hence velocity gradients), more cholesterol is washed away by the blood flow. On the other hand, where the shear stress is low, excess cholesterol is deposited on the surface of the lumen initiating atheroma development (caro et al. [19], Layek et al. [20]). So it is very important to notice the wall shear stress distribution in the constricted region. So wall shear stress near the throat of the constriction deserves special attention. It is observed that the peak value of wall shear stress is higher in Newtonian case than that of non-Newtonian case, which is presented in Fig. 4.

For the physiological values of blood (i.e. λ=14.72 and Λ=14.81), the time-dependent wall shear stress distributions are exhibited in Fig. 5(a)-(c) for various Strouhal number (*st)* at fixed Reynolds number *Re*=100. It is observed that the peak value of the shear stress increases with *st* and flow separation starts at the throat of the stenosis at t=0.50.

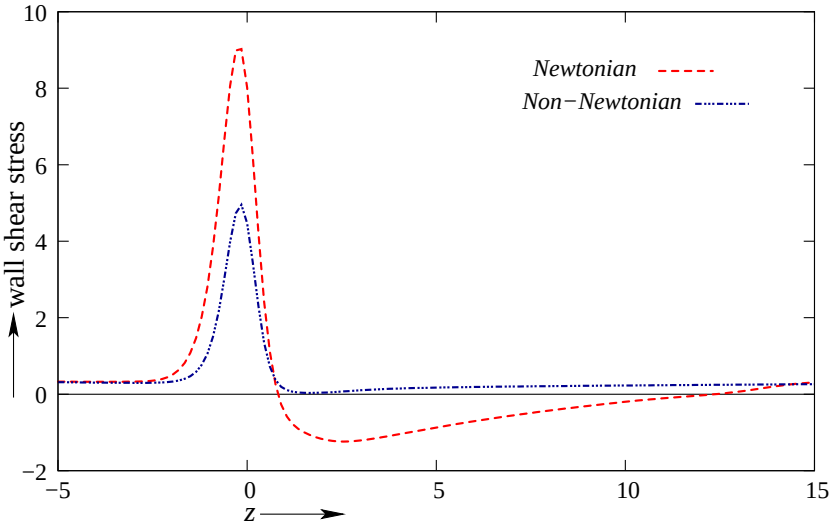

Figure 4: The wall shear stress distribution under sinusoidal flow rate condition for both Newtonian and non-Newtonian cases at $t = 0.5, Re = 100$ and $st = 0.06$.

At time t=0.60 the peak value of the wall shear stress decreases compared to the previous case and large separation region is formed at down stream. Length of separation increases with increasing st. Larger separation zone at st=0.09 indicates the presence of strong eddy in the downstream. This means that at t=0.60 shear stress is negative in down stream direction and a flow separation region is growing. At t=0.75 the wall shear stress is completely negative and the flow separation region is continuously increasing. The negative values of wall shear stress indicate the separating region and is substantially more prevalent than the positive values because of separation. Separation of the boundary layer gives rise to the flow structure which has important implications in understanding and predicting the flow characteristics. Moreover, the extent of the negative shear stress region gives an idea about the size of the re-circulation eddies. The re-circulation zone indicates the region where the flow is reversed. Thus, appearance of these re-circulation regions is of pathological significance since, these are regions of low shear and may prolong the residing time of blood constituents that can eventually pass into the arterial wall.

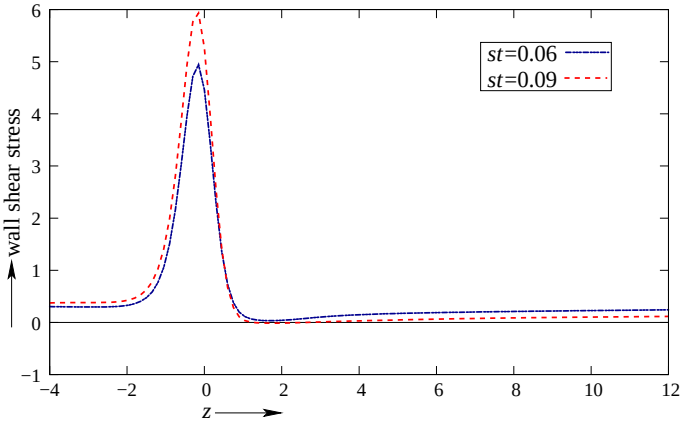

(a) $t = 0.50$

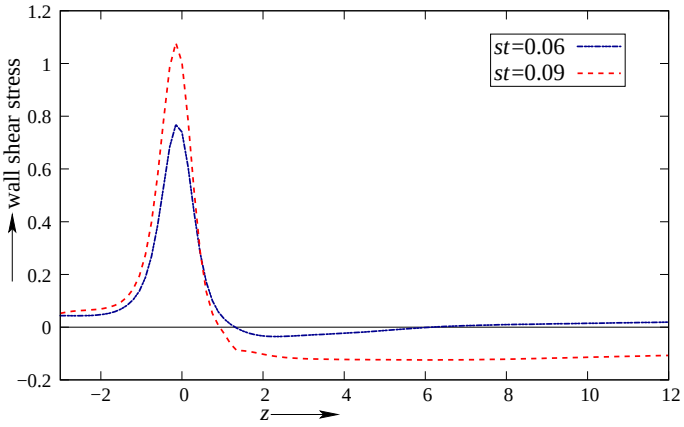

(b) $t = 0.60$

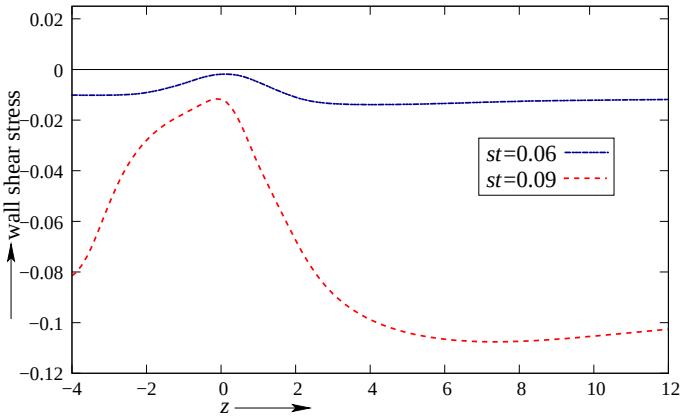

(c) $t = 0.75$

Figure 5: The wall shear stress distribution under sinusoidal flow rate condition for $Re = 100$ and for different st at diverse t

The wall shear stresses at t=0.50 for different values of Reynolds number $Re$is presented in Fig.6. It reveals that the peak value of wall shear stress increases

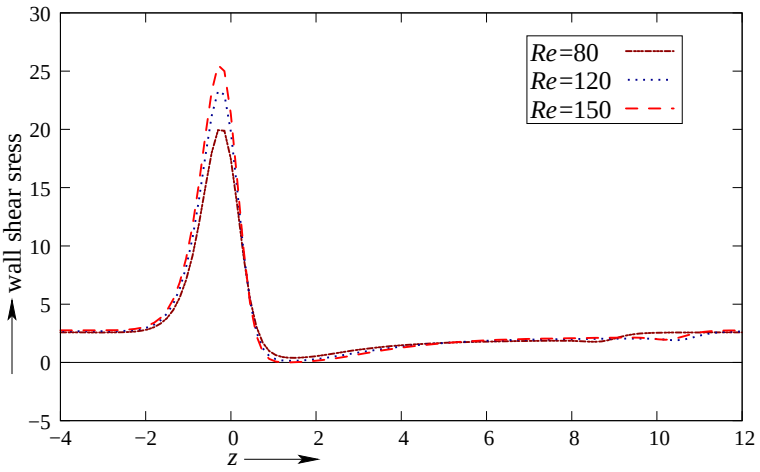

Figure 6: The wall shear stress distribution under sinusoidal flow rate condition for different Re at $t = 0.50$ and $st = 0.06$.

for increasing Reynolds number Re. The peak of the shear stress is believed to cause severe damage to the arterial lumen which in turn helps in detecting the aggregation sites of platelets may have several consequences in circulatory system.

Next, we pay our attention to analyse the flow characteristics, particularly the wall shear stress due to pulsatile flow rate. For this we have consider physiologically relevant pulsation as given by

$$\begin{aligned} f(t) = {} & 0.4355 + 0.05\cos(2\pi t) + 0.25\sin(2\pi t) - 0.13\cos(4\pi t) \\ & + 0.13\sin(4\pi t) - 0.10\cos(6\pi t) - 0.02\sin(6\pi t) \\ & - 0.01\cos(8\pi t) - 0.03\sin(8\pi t) \end{aligned}$$

and the effects of pulsatile flow rate on wall shear stress are exhibited in Fig. 7(a)-(c) for three different time stations and st numbers. From Fig. 7(a), it is very clear that flow separation occurs at earlier time for both the st has at the Re=100. Fig. 7(b) represents the fluctuating nature of wall shear stress in the separated region.

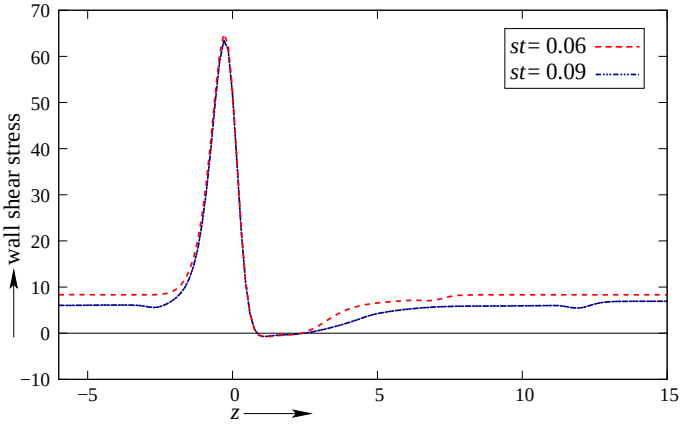

(a) $t = 0.18$

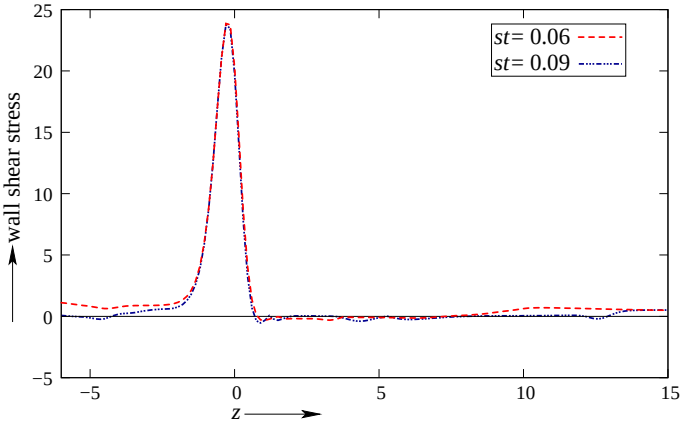

(b) $t = 0.30$

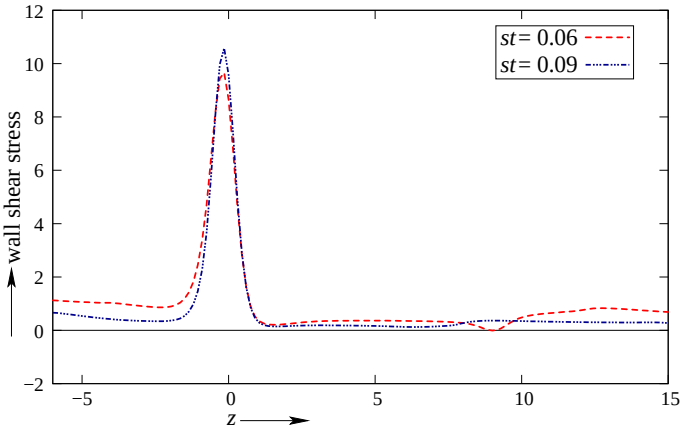

(c) $t = 0.39$

Figure 7: The wall shear stress distribution under physiological pulsatile flow rate condition for $Re = 100$ and for different st at diverse t.

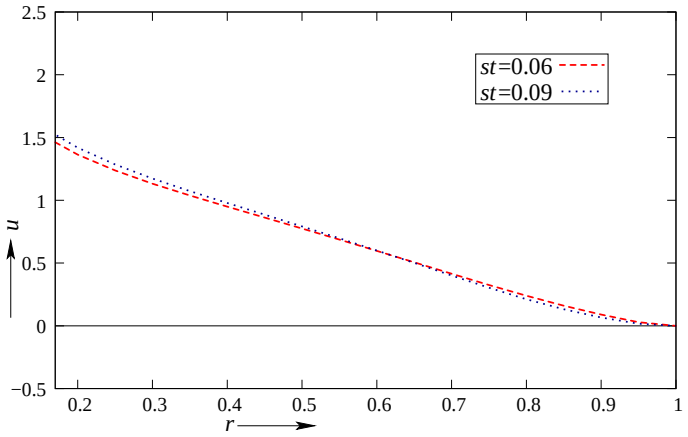

(a) $t = 0.50$

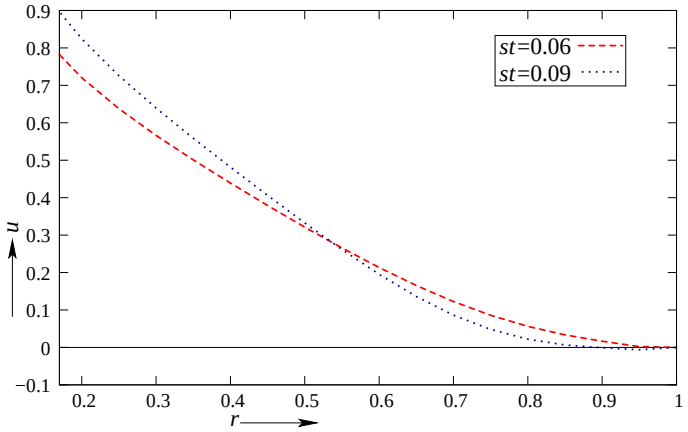

(b) $t = 0.60$

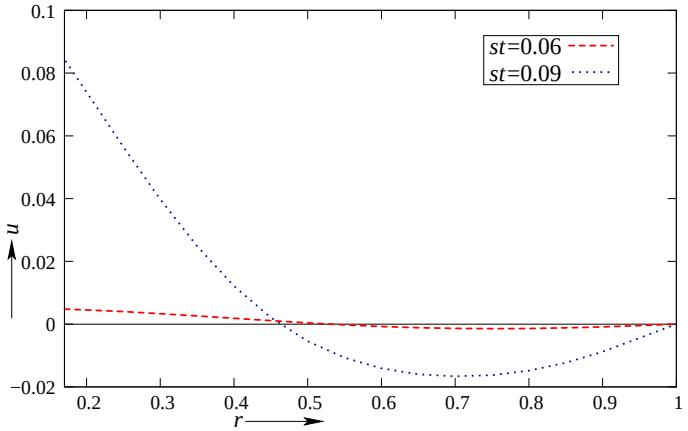

(c) $t = 0.75$

Figure 8: The velocity profile under sinusoidal flow rate condition for $Re = 100$ and for different st at diverse t.

Table 1: Result of stream-function$\psi$and vorticity $\omega$for a long straight circular tube at $Re = 10$, $st = 1$.

R	0.0	0.25	0.50	0.75	1.0
ψ	0.0	0.03027	0.109838	0.20215	0.25002
Exact ψ	0.0	0.03027	0.109838	0.20215	0.25000
ω	0.0	0.49977	0.99514	1.49622	1.99323
Exact ω	0.0	0.50000	1.00000	1.50000	2.00000

However upstream separation is noted for st=0.09 at t=0.30 at Re=100. This result is of great physiological importance. After a later time i.e. at t=0.39, no separation is noted [Fig. 7(c)]. The velocity profiles are of some interest as they provide a detailed description of the flow field. The velocity profile are shown at different time location for fixed Re=100 and for various value of Strouhal number (st). in Fig. 8(a)-(c).

At t=0.60 and t=0.75 the region of reversal flow is evident in these figures. In this region i.e. the back flow region, the component of velocity undergoes a change in sign. Fig. 9 displays the nature of velocity profiles for different values of Reynolds number (Re) at time t=0.50.

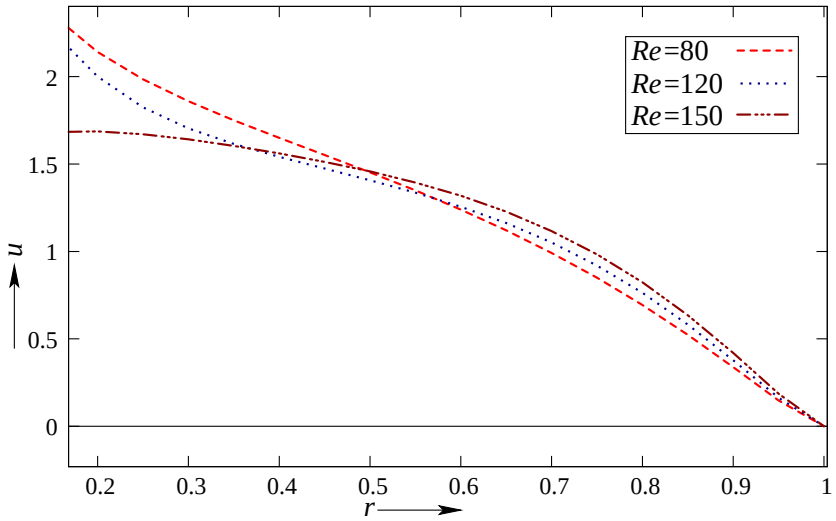

Figure 9: The velocity profile under sinusoidal flow rate condition for st = 0.06 and for different Re at $t = 0.50$.

6 Conclusions

A numerical simulation of pulsatile blood flow with shear dependent viscosity through a modeled artery with bell-shaped constriction is carried out for sinusoidal and physiological flow rate separately. The main findings of this study are summarised as follows:

(i) Viscosity increases with increasing the parameterλ, but decreases with increasing the parameterΛ.

(ii) The peak value of wall shear stress is larger in physiological flow rate than the sinusoidal flow rate.

(iii) Length of separation is larger in sinusoidal flow rate than that of the physiological flow rate.

Therefore it can be concluded that the non-Newtonian character of blood can modify the flow pattern and may have some biomedical application.

Acknowledgement:

The authors are thankful to the reviewer for their constructive suggestions which helped a lot for the improvement of the quality of the paper.

References

[1] D.F. Young, F.Y. Tsai, Flow characteristics in models of arterial stenosis –I. Steady Flow, J. Biomechanics, 6, (1973), 395-410.

[2] D.F. Young, F.Y. Tsai, Flow characteristics in models of arterial stenosis –II. Unsteady Flow, J. Biomechanics, 6, (1973), 554-559.

[3] M. Siouffi, R. Pelisser, D. Farahifar, R. Rieu, The effect of unsteadiness on the flow through stenoses and Bifurcation, J.Biomechanics, 17, (1984), 299-315.

[4] D.N. Ku, Blood flow in arteries, Annu. Rev. Fluid Mech., 29, (1997), 399-434.

[5] C.G. Caro, T.J. Pedley, R.C. Schroter, W.A. Seed, The mechanics of the circulation, New York, Oxford Medical, 1978.

[6] M. Nakamura, T. Sawada, Numerical study on flow of non-Newtonian fluid through axi-symmetric stenosis, J .Biomech. Eng., 110, (1988), 247-262.

[7] G.C. Layek, C. Midya, Effect of constriction hight on flow separation in a two-dimensional channel, Commun. Nonlinear Sci. Numer. Simul., 12, (2007), 745-759.

[8] G. Pedrizzetti, Unsteady tube flow over an expansion, J. Fluid Mech., 310, (1996), 89-111.

[9] R. Mittal, S.P. Simmons, F. Najjar, Numerical study of pulsatile flow in a constricted channel, J. Fluid Mech., 485, (2003), 337-378.

[10] O.R. Tutty, Pulsatile flow in a constricted channel, J. Biomech. Eng., 114, (1992), 50-54.

[11] O.R. Tutty, T.J. Pedley, Oscillatory flow in a stepped channel, J. Fluid Mech., 247, (1993), 179-204.

[12] R.E. Nerem, Vascular fluid mechanics, the arterial wall and arteriosclerosis, Journal of Biomechanical Engineering Transactions ASME, 114, (1992), 274–282.

[13] M. Anand, K.R. Rajagopal, A shear-tinning viscoelastic fluid model for describing the flow of blood, Int. J. Cardiovascular Medicine Sci., 4, (2004), 59-68.

[14] K.K. Yeleswarapu, M.V. Kameneva, K.R. Rajagopal, J.F. Antaki, The flow of blood in tubes: theory and experiments, Mech. Res. Commun., 25, (1998), 257-262.

[15] K.K. Yeleswarapu, Evaluation of continuum models for characterizing the constitutive behavior of blood, Ph.D. thesis, University of Pittsburgh, 1996.

[16] G.K. Batchelor, An Introduction to Fluid Dynamics, Cambridge University Press, 1967.

[17] R. Peyret and T.D. Taylor, Computational Methods for fluid Flow, Springer-Verlag, 1982.

[18] G. Pontrelli, Blood flow through axisymmetric stenosis, Proc. Inst. Mech. Eng. Part H. J. Eng. in Medicine., 215, (2001), 1-10.

[19] C. G. Caro, J. M. Fitzgerald and R. C. Schroter, Atheroma and arterial wall shear observation: correlation and proposal shear dependent mass transfer mechanism for atherogenesis, Proc. Roy. Soc. Med. London, Ser. B, 177, (1971), 109–159.

[20] G. C. Layek, S. Mukhopadhyay and Sk. A. Samad, Oscillatory Flow in a Tube with Multiple Constrictions, International Journal of Fluid Mechanics Research, 32 (4), (2005), 402-419.

Submitted in July 2011.

Pulzatorno strujanje fluida u zavisnosti od smicanja u arteriji sa suženjem

Cilj istraživanja u ovom radu je strujanje krvi u krutoj cevi oblika zvona kojim se modelira arterija sa suženjem. Pretpostavka za strujanje fluida je da je osnosimetrično, laminarno i oscilatornog tipa. Razmatra se matematički model fluida u smičućem sloju koji odgovara zavisnosti viskoznosti od smicanja (uglavnom zbog mešavine crvenih krvnih zrnaca u krvi). Odgovarajuće jednačine kretanja su opisane sa korišćenjem strujne funkcije vrtloga i rešavane numerički metodom konačnih razlika. Model fluida sa smičućom funkcijom zavisnosti ima značajan uticaj na dinamiku oscilatornog strujanja. Dobijeni rezultati su pokazali da se arterijski smičući napon smanjuje značajno i da se vrednosti maksimalnog smičućeg napona na maksimalnom suženju niži u odnosu na Njutnov viskozni fluid. Dužine recirkularnih oblasti koje se formiraju posle suženja su manje za viskozno zavisni smičući fluidni model i takodje za njegove različite materijalne parametre.

doi:10.2298/TAM1203209M Math.Subj.Class.: 74L15, 92C10